

William Barker

New program for uncertainty in PCD measurements using Monte Carlo method compatible with Sinton WCT-120 lifetime tester.

William Barker¹, Andrew Thomson¹

¹*Research School of Engineering, The Australian National University (ANU), Canberra 0200, Australia*

E-mail: u5009574@anu.edu.au

Abstract

A new program for calculation of uncertainties in a photoconductance decay measurement has been developed in Excel. The program is designed for use with Sinton WCT-120 Lifetime Tester software, and will shortly be downloadable from PVLighthouse.com.au. The major feature of the program is the inclusion of the calibration in the conductivity-voltage relationship in the Monte Carlo method variable parameters list. This is achieved through a quadratic fit of the uncertainty in the conductivity as a function of voltage. Initial results of the program show reasonable agreement with the work of (Thomson, Hameiri *et al.* 2013).

1. Introduction

Contactless photoconductance decay (PCD) measurements were first proposed in the seminal work (Kane and Swanson 1985). Since then, the technique has become a standard method for analysis of the quality of the surface of a sample. The development of Quasi-Steady State PCD, outlined in (Sinton and Cuevas 1996) was a major improvement in the technique, allowing much higher injection levels to be realised in the measurements. Since 1996, the technique has become a standard in the determination of surface and bulk recombination properties of silicon wafers (King, Sinton *et al.* 1990; King and Swanson 1991; Kerr and Cuevas 2002; Richter, Glunz *et al.* 2012).

The main advantages of the PCD technique are:

1. It is very fast (taking less than 1 second to complete the measurement)
2. It is non-destructive to the sample
3. The equipment is relatively cheap

Photoconductance decay measurements consist of exposing a sample to a short flash, and then measuring the number of excited carriers in the sample over time. To measure the number of carriers, the conductivity of the sample (a known function of the number of charge carriers in the sample) is measured via an induction coil under the sample. The voltage measured by the induction coil is proportional to the conductivity of the sample.

From the PCD measurement, the effective lifetime can be calculated as a function of injection level, and from this the recombination parameter J_0 can be calculated. The traditional method of this calculation (still used in the WCT-120 Sinton software) is to use Equation 1 (Kane and Swanson 1985).

$$J_0 = \frac{1}{2} q W n_i^2 \frac{d}{d\Delta n} \left(\frac{1}{\tau_{corr}} \right) \quad (1)$$

where W is the thickness of the sample, q is the elementary charge, τ_{corr} is the Auger corrected lifetime, n_i is the intrinsic carrier concentration and Δn is the density of excess charge carriers.

Equation 1 assumes that the intrinsic carrier concentration is independent of the injection level. This assumption ignores the effect of Band Gap Narrowing at high injection levels. As such, a recent improvement on the technique has been proposed in (Kimmerle, Greulich *et al.* 2015), based on the work of (Sproul 1994). Instead of using Equation 1 to calculate J_0 , Kimmerle, Greulich *et al.* propose the use of Equation 2.

$$J_0 \approx \frac{qW}{2} \frac{d}{d\Delta n_{av}} \left(\frac{n_{i,eff}^2}{\tau_s - \frac{W^2}{D\pi^2}} \right) \quad (2)$$

where Δn_{av} is the average density of excess charge carriers across the sample, D is the ambipolar diffusion coefficient, τ_s is the surface recombination lifetime (see Kimmerle, Greulich *et al.* for further discussion) and $n_{i,eff}$ is the effective carrier concentration given by Equation 3 (Richter, Glunz *et al.* 2012)

$$n_{i,eff} = n_i e^{\Delta E_g / 2kT} \quad (3)$$

where k is the Boltzmann constant, T is the Temperature and ΔE_g is the amount by which the band gap has narrowed (measured in eV), given by the Schenk model (Schenk 1998).

Kimmerle, Geulich *et al.* have reported that using Equation 2 in place of Equation 1 (in combination with a novel technique to solve for the Shockley Read Hall recombination) yields a dramatic improvement in the stability of the calculated J_0 over a range of injection levels. Additionally, the accuracy of the calculated J_0 values from numerical simulations is much better for Equation 2.

With this improved technique, and more accurate determination of J_0 , a natural progression is to try to understand the uncertainty in the calculated value. As the J_0 of a sample is a complicated function of the input variables, analytical determination of the uncertainty from the uncertainty in the input parameters is not possible. As such, Monte Carlo method (MCM) simulations are a very powerful technique to determine the uncertainties in the outputs of the measurements (Papadopoulos and Yeung 2001; JCGM-101:2008 2008).

This work describes a new program for estimation of uncertainty in PCD measurements using the Monte Carlo method compatible with Sinton WCT-120 Lifetime tester.

2. Program Description

The program developed by the author is available in Microsoft Excel, which allows it to easily integrate with the existing Sinton WCT-120 Lifetime Tester software. The program presents an intuitive user interface, similar to that of the Sinton software. The main function

of the software is to take input parameters with uncertainties from the user, vary these in the Sinton spreadsheet, and extract user specified outputs for these inputs. The program will be available for download from PVLighthouse.com.au in the near future.

The method implemented by the program to conduct the uncertainty analysis builds on the work of (Thomson, Hameiri *et al.* 2013), and extends it in two respects:

1. Making the technique accessible, by creating a program in Excel
2. Extending the inputs to include the calibration of the measured voltage in the induction coil with the conductivity of the sample.

The estimation of the uncertainty in the inputs is calculated via a Monte Carlo sampling approach. This entails independent variation of each desired parameter by a random number of standard deviations (i.e. the uncertainty) from the average value. The random number is sampled from a Gaussian distribution of standard deviation 1 and mean 0. This process is repeated a user-defined number of times, typically of the order of 100 is appropriate, although occasionally $\sim 10^4 - 10^5$ can be necessary (Thomson, Hameiri *et al.* 2013). For each loop, the input value of each input variable is varied in the way described above, and inserted into the Sinton spreadsheet. The typical input variables are:

- Wafer Thickness, W ;
- The doping concentration, N_{dop} ;
- Specified Minority Carrier Density, MCD ;
- The Optical Constant, OC .

The typical output variables are J_0 and the effective carrier life time, τ_{eff} , at the specified MCD.

In addition to the above input parameters, the program includes the novel ability to include the calibration of the voltage, V , to conductivity, S , in the MCM parameter variation. This builds on the work of Thomson, Hameiri *et al.* but extends it to allow for seamless integration with the MCM program and Sinton WCT-120 lifetime tester software.

In the Sinton WCT-120 lifetime tester spreadsheet software, the conductivity of the wafer is modelled as a quadratic function of the measured voltage in the induction coil. This leads to the determination of three parameters, called A , B and C in the Sinton spreadsheet. These three values are correlated, and hence cannot be individually varied inside the spreadsheet. Instead, it is required to analyse the calibration data, and determine the relationship between the three constants.

In order to understand how to calculate the uncertainty in the calibration, it is necessary to understand how the Sinton spreadsheet calculates the conductivity from the voltage. To do this, the machine first needs to be calibrated using several wafers of known conductivity in the dark. The calibration wafers are placed on top of the induction coil, and the voltage in the coil is measured, and recorded along with the conductivity of the wafer. The spreadsheet then assumes a quadratic relationship between the two variables, i.e. Equation 4.

$$S_i = AV_i^2 + BV_i + C \quad (4)$$

where S_i and V_i are the measured conductivity and voltage of the i -th wafer respectively. When multiple wafers are used for calibration, a series of equations are generated, which can be expressed as the matrix Equation 5.

$$\mathbf{V}\mathbf{b} = \mathbf{S} \quad (5)$$

$$\text{where } \mathbf{S} = \begin{pmatrix} S_1 \\ \vdots \\ S_n \end{pmatrix} \quad \mathbf{V} = \begin{pmatrix} V_1^2 & V_1 & 1 \\ \vdots & \vdots & \vdots \\ V_n^2 & V_n & 1 \end{pmatrix} \quad \text{and } \mathbf{b} = \begin{pmatrix} A \\ B \\ C \end{pmatrix}$$

The accuracy of Equation 4 can be seen by the plot of S against V for the calibration data plotted in Figure 1.

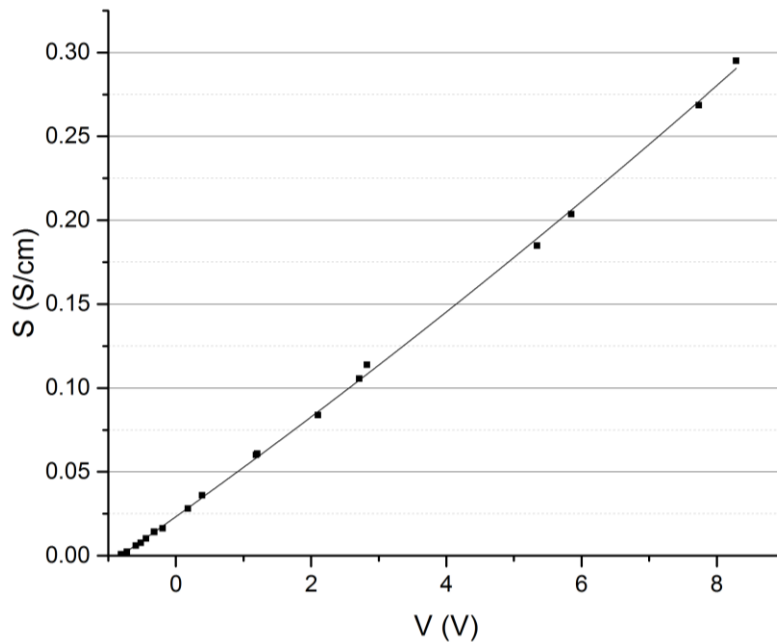


Figure 1. Plot of conductivity against measured voltage in induction coil, with quadratic line of best fit.

Equation 5 is then solved for \mathbf{b} , by first multiplying both sides from the left by \mathbf{V}^T (as $\mathbf{V}^T\mathbf{V}$ is a square matrix, where \mathbf{V} need not be, and hence, its inverse is not defined), resulting in Equation 6.

$$\mathbf{V}^T\mathbf{V}\mathbf{b} = \mathbf{V}^T\mathbf{S} \quad (6)$$

\mathbf{b} is then easily calculated by calculating the inverse of $\mathbf{V}^T\mathbf{V}$, and then multiplying both sides of Equation 6 by this, yielding Equation 7.

$$\mathbf{b} = (\mathbf{V}^T\mathbf{V})^{-1}\mathbf{V}^T\mathbf{S} \quad (7)$$

To calculate the uncertainty in the value of S calculated using the above value for \mathbf{b} , it is necessary to calculate the variance of \mathbf{b} , as the uncertainty is given by Equation 8.

$$\sigma_{S,i} = \sqrt{\begin{pmatrix} V_i^2 & V_i & 1 \end{pmatrix} \cdot \text{var}(\mathbf{b}) \cdot \begin{pmatrix} V_i^2 \\ V_i \\ 1 \end{pmatrix}} \quad (8)$$

where $\sigma_{S,i}$ is the uncertainty in the calculated conductivity of the i -th calibration measurement, and the variance of \mathbf{b} is given by Equation 9 (G.E.P. Box 1978).

$$\text{var}(\mathbf{b}) = (\mathbf{V}^T \mathbf{V})^{-1} \text{var}(\mathbf{S}) \quad (9)$$

and the variance of \mathbf{S} is given by Equation 10 (G.E.P. Box 1978).

$$\text{var}(\mathbf{S}) = \frac{(\mathbf{V}\mathbf{b} - \mathbf{S})(\mathbf{V}\mathbf{b} - \mathbf{S})^T}{(n-3)} \quad (10)$$

where n is the number of measurements, or the number of entries in the \mathbf{S} vector, and the factor of 3 arises to make the measurement unbiased, because of the 3 degrees of freedom in the problem (the A , B and C parameters).

The next step is the novel component of this method. This involves analysis of the $\sigma_{S,i}$ against V plot, as shown in Figures 2 and 3. It is apparent from these Figures that the $\sigma_{S,i}$ can be smoothly fitted as a quartic function of V , but can be well approximated as a quadratic. In the program, the latter fit is used.

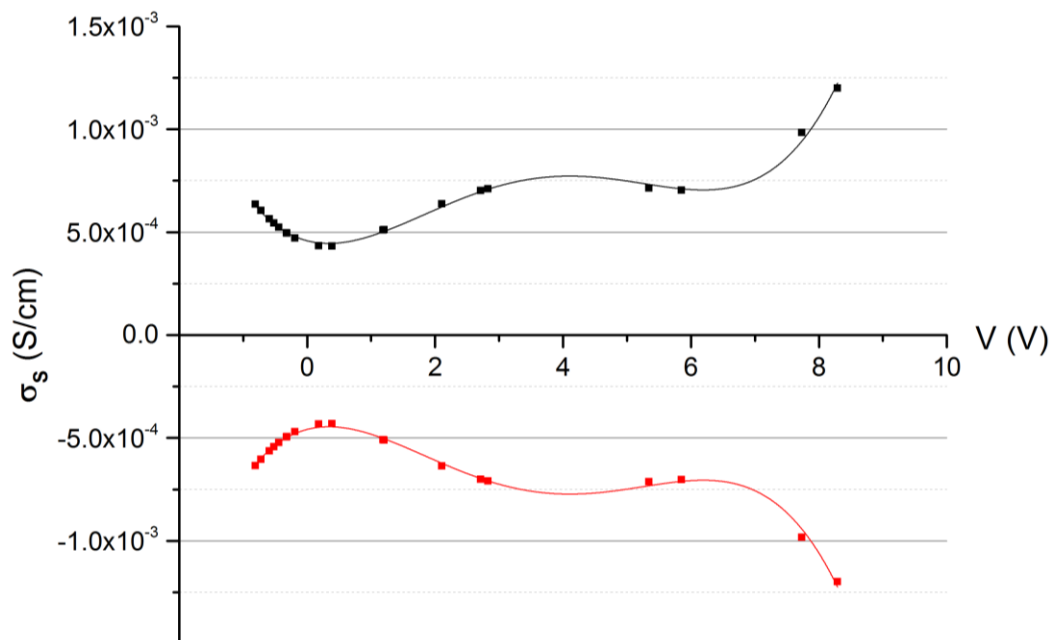


Figure 2. Quartic fit of Uncertainty in conductivity against measured voltage in induction coil.

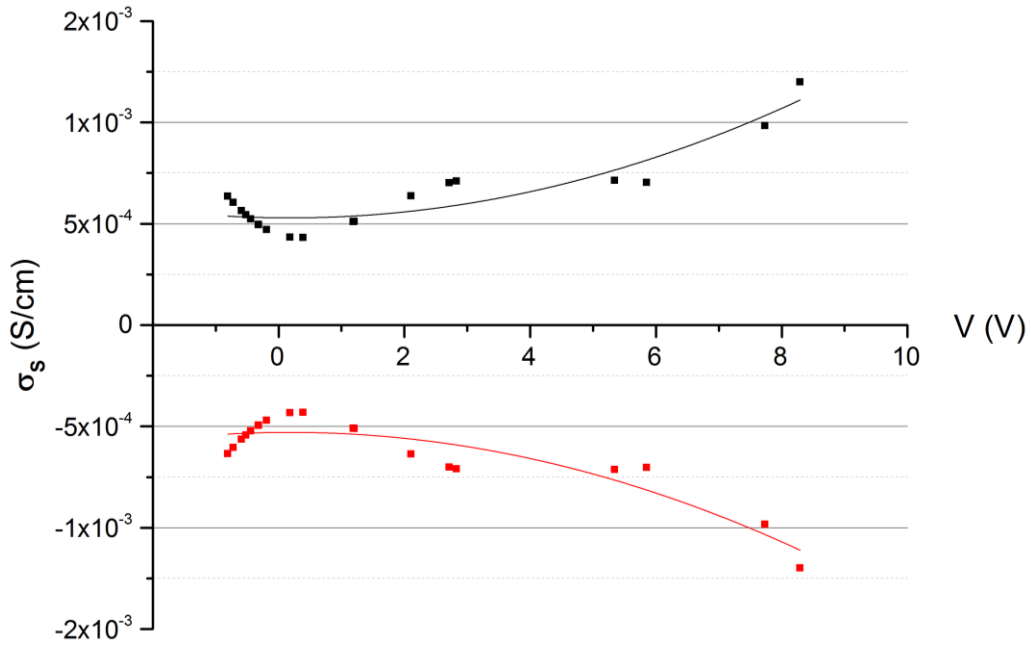


Figure 3. Quadratic fit of uncertainty in conductivity against measured voltage in induction coil.

From the values of $\sigma_{S,i}$ the vector $\boldsymbol{\sigma}_s = \begin{pmatrix} \sigma_{S,1} \\ \vdots \\ \sigma_{S,n} \end{pmatrix}$ can be defined, and from it the vector $\boldsymbol{\sigma}_b$, defined by Equation 11.

$$\mathbf{V}(\mathbf{b} \pm \boldsymbol{\sigma}_b) = (\mathbf{S} \pm \boldsymbol{\sigma}_s) \quad (11)$$

It is apparent from this definition that $\boldsymbol{\sigma}_b$ contains the uncertainties in the calibration constants required for inclusion of the calibration uncertainty in the MCM analysis. In fact,

$\boldsymbol{\sigma}_b$ can be expressed as $\boldsymbol{\sigma}_b = \begin{pmatrix} \sigma_A \\ \sigma_B \\ \sigma_C \end{pmatrix}$, where σ_A is the uncertainty in A , σ_B is the uncertainty in B and σ_C is the uncertainty in C .

From Equation 11, the obvious simplification to Equation 13 can be performed, using Equation 5.

$$\mathbf{V}\mathbf{b} \pm \mathbf{V}\boldsymbol{\sigma}_b = \mathbf{S} \pm \boldsymbol{\sigma}_s \quad (12)$$

$$\Rightarrow \mathbf{V}\boldsymbol{\sigma}_b = \boldsymbol{\sigma}_s \quad (13)$$

Using Equation 13 a very convenient method for calculation of $\boldsymbol{\sigma}_b$ is apparent by analogy with the process described above for Equation 5, leading to Equation 14.

$$\boldsymbol{\sigma}_b = (\mathbf{V}^T \mathbf{V})^{-1} \mathbf{V}^T \boldsymbol{\sigma}_s \quad (14)$$

This Equation is then solved in the program, to give a value of σ_b . This value is then subsequently substituted back into Equation 11, and the values of $V(\mathbf{b} \pm \sigma_b) - \mathbf{S}$ are calculated and compared against the original values of $\pm \sigma_s$. An example of this comparison is shown in Figure 4. In this Figure, the data points represent the value of $((A + \sigma_A)V_i^2 + (B + \sigma_B)V_i + (C + \sigma_C)) - S_i$, whilst the dashed line is the quadratic fit from Figure 3. As is required by the definition of σ_b in Equation 11, the quadratic line of best fit from Figure 3 fits the data calculated from σ_b extremely well, which is clear from Figure 4. Figure 4 is reproduced (along with select other plots) in the program to allow the user to check that the calculation of σ_b from the input calibration measurements is accurate.

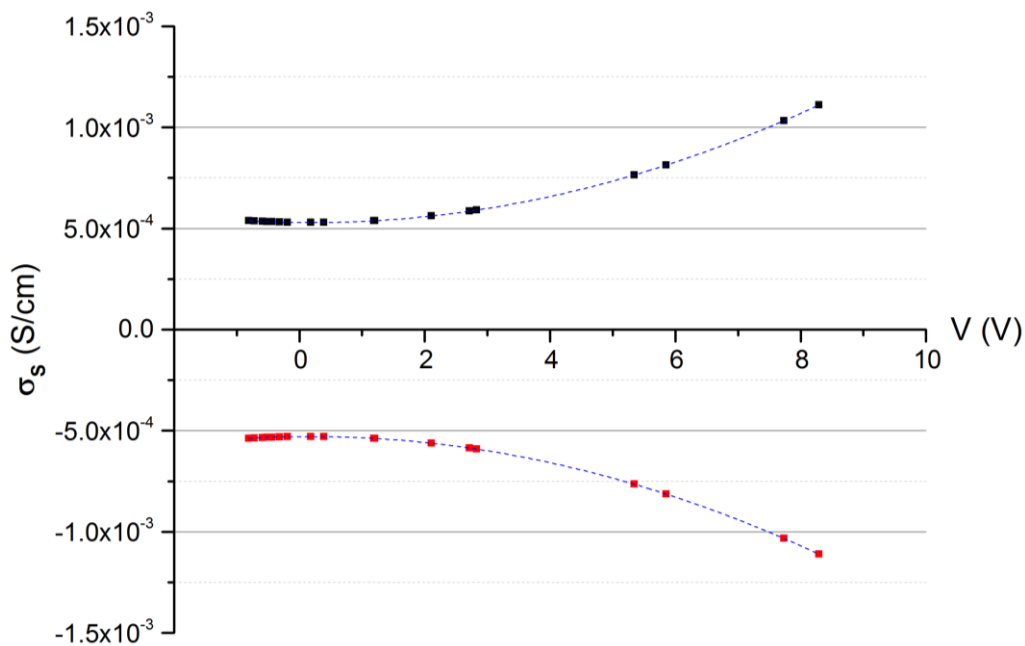


Figure 4. Plot of uncertainty as calculated from (dots) Equation 13 using σ_b from Equation 14 and (line) quadratic fit of σ_s from Equation 8.

3. Program Results/ Validation

As an initial test to prove the functionality of the program, the data from four existing QSS PCD measurements was analysed to determine uncertainties. The samples in question are described in (Thomson, Hameiri *et al.* 2013). These samples were selected, as existing data on the uncertainties in these samples already existed, and thus, they are good point of reference to determine the accuracy of the new program. Only QSS measurements were included in the MCM analysis presented here, because the work of (Kimmerle, Greulich *et al.* 2015) only applies to QSS measurements, and has not yet been generalised to transient measurements. Hence, currently, these are the measurements of most interest. The input parameters to be varied, with their uncertainties, for each of the four samples is shown in Table 1.

Table1. Summary of input parameters with uncertainties for initial QSS analysis of impact of Calibration inclusion in MCM analysis.



| Sheet Res. (Ω/sq) | W (μm) | N ($\times 10^{14} \text{ cm}^{-3}$) | MCD ($\times 10^{15} \text{ cm}^{-3}$) | OC |
|--------------------------------------|------------------------|---|---|-----------------|
| 32 | 527 ± 8 | 1.1 ± 0.2 | 2 ± 0.4 | 0.72 ± 0.01 |
| 40 | 526 ± 8 | 1.1 ± 0.2 | 2 ± 0.4 | 0.72 ± 0.01 |
| 68 | 518 ± 9 | 1.1 ± 0.2 | 2 ± 0.4 | 0.70 ± 0.02 |
| 130 | 537 ± 15 | 1.1 ± 0.2 | 2 ± 0.4 | 0.69 ± 0.01 |

In accordance with (Thomson, Hameiri *et al.* 2013), 4000 runs were conducted for each sample shown in Table 1, to build up sufficient statistics. Each sample was tested 3 times, and the results found to be very consistent, as shown in Table 2, along with the values determined for the samples by (Thomson, Hameiri *et al.* 2013). The S-V calibration was not included as an input parameter of variation for these samples, as the S-V calibration data was not available for the samples tested.

Table2. Initial results of new program on samples prepared for (Thomson, Hameiri *et al.* 2013) using inputs described in Table 1 without S-V calibration inclusion in MCM.

| Sheet Res. (Ω/sq) | Run Number | J_0 (fA/cm^2) | |
|--------------------------------------|---------------|-----------------------------------|--|
| | | Calculated by new program | (Thomson, Hameiri <i>et al.</i> 2013) |
| 32 | 1 | 243 ± 2 | 235 ± 9 |
| | 2 | 242 ± 2 | |
| | 3 | 243 ± 2 | |
| 40 | 1 | 291 ± 2 | 293 ± 12 |
| | 2 | 291 ± 2 | |
| | 3 | 291 ± 3 | |
| 68 | 1 | 174 ± 2 | 166 ± 9 |
| | 2 | 174 ± 2 | |
| | 3 | 174 ± 2 | |
| 130 | 1 | 124 ± 2 | 114 ± 7 |
| | 2 | 125 ± 2 | |
| | 3 | 124 ± 2 | |

The results from Table 2 show that the values calculated by the new program differ from the values calculated by (Thomson, Hameiri *et al.* 2013). This is primarily because the range of MCD values over which the results in the reference was averaged was much larger than those used in this paper. Additionally the uncertainties in the calibration were included in (Thomson, Hameiri *et al.* 2013), which was not possible for these samples. However, it is clear from above that the program shows good initial results, but further testing is still required.

4. Conclusion

A new program for determination of the uncertainty of results of a PCD measurement developed by the author is described. This program includes the novel ability to add the calibration constants for the PCD measurement as inputs in the MCM analysis.

An initial investigation into the accuracy of the program shows good potential. Noticeable difference between the results of (Thomson, Hameiri *et al.* 2013) and the results of the program exist, but these can be explained by differences in the input parameters. Further measurements are required to fully test the program, and the novel conductivity-voltage calibration inclusion in the MCM.

References

G.E.P. Box, W. G. H. a. J. S. H. (1978). Statistics for Experimenters: An Introduction to Design, Data Analysis and Model Building. Hoboken, NJ, Wiley.

JCGM-101:2008 (2008). Evaluation of measurement data — Supplement 1 to the “Guide to the expression of uncertainty in measurement” — Propagation of distributions using a Monte Carlo method, BIPM, IEC, IFCC, ILAC, ISO, IUPAC, IUPAP, OIML.

Kane, D. and R. Swanson (1985). Measurement of the emitter saturation current by a contactless photoconductivity decay method. IEEE photovoltaic specialists conference. 18.

Kerr, M. J. and A. Cuevas (2002). "General parameterization of Auger recombination in crystalline silicon." Journal of Applied Physics **91**(4): 2473-2480.

Kimmerle, A., J. Greulich, et al. (2015). "Carrier-diffusion corrected J₀-analysis of charge carrier lifetime measurements for increased consistency." Solar Energy Materials and Solar Cells **142**: 116-122.

King, R. R., R. A. Sinton, et al. (1990). "Studies of diffused phosphorus emitters: saturation current, surface recombination velocity, and quantum efficiency." IEEE Transactions on Electron Devices **37**: 365-371.

King, R. R. and R. M. Swanson (1991). "Studies of diffused boron emitters: saturation current, bandgap narrowing, and surface recombination velocity." IEEE Transactions on Electron Devices **38**(6): 1399-1409.

Papadopoulos, C. E. and H. Yeung (2001). "Uncertainty estimation and Monte Carlo simulation method." Flow Measurement and Instrumentation **12**(4): 291 - 298.

Richter, A., S. W. Glunz, et al. (2012). "Improved quantitative description of Auger recombination in crystalline silicon." Physical Review B **86**(16): 165202.

Schenk, A. (1998). "Finite-temperature full random-phase approximation model of band gap narrowing for silicon device simulation." Journal of Applied Physics **84**(7): 3684-3695.



2015 ASIA-PACIFIC SOLAR RESEARCH CONFERENCE

Sinton, R. A. and A. Cuevas (1996). "Contactless determination of current–voltage characteristics and minority-carrier lifetimes in semiconductors from quasi-steady-state photoconductance data." Applied Physics Letters **69**(17): 2510-2512.

Sproul, A. (1994). "Dimensionless solution of the equation describing the effect of surface recombination on carrier decay in semiconductors." Journal of Applied Physics **76**(5): 2851-2854.

Thomson, A. F., Z. Hameiri, et al. (2013). "Uncertainty in photoconductance measurements of the emitter saturation current." Photovoltaics, IEEE Journal of **3**(4): 1200-1207.